Spector: integration and performance of the multi-object spectrograph for the Anglo-Australian Telescope

Ross Zhelem[*a,c], Julia Bryant[b,c], Joss Bland-Hawthorn[b,c], Rebecca Brown[a,c], Robert Content[a,c], Scott Croom[b,c], Tony Farrell[a,c], Michael Goodwin[a,c], Ellen Houston[a,c], Urs Klauser[a,c], Jon Lawrence[a,c], Slavko Mali[a,c], Rolf Muller[a,c], Richard McDermid[a,c], Helen McGregor[a,c], Mahesh Mohanan[a,c], Barnaby Norris[b,c], Naveen Pai[a,c], David Robertson[a,c], Will Saunders[a,c], Lew Waller[a,c], Adeline Wang[b,c], Jessica Zheng[a,c]
[a] Australian Astronomical Optics, Macquarie University, Australia; [b] Sydney Institute for Astronomy, The University of Sydney, Australia ; [c] Astralis Instrumentation Consortium, Australia

ABSTRACT

The Hector instrument was installed at the Anglo-Australian Telescope in December 2021. All major subsystems, namely, the positioner, spectrograph and optical cable, performed as expected and the instrument received the first light. Spector is the new spectrograph with an average spectral resolution of R=4500 complementing the existing lower resolution AAOmega facility. Instrument design was optimized for hexabundles, the integral field units capturing telescope output. Fibers are arranged along a curved slit and a spherical focal surface at precise spacing to minimize cross talk. Details of the integration and testing of the spectrograph optics are presented here. Optical elements were manufactured externally, then aligned and assembled in-house. The spectrograph cameras work with an 180 mm pupil in a fast F/1.3 beam. Extreme sensitivity to errors requires lens positioning to 10 micron accuracy in decenter. The detector windows are aspheric and tilted and decentered with respect to the optical axis of the cameras. An alignment procedure was developed to measure and correct critical parameters of the system. Precision alignment is implemented in the lab, each optics mounts on the instrument structure kinematically allowing quick installation at a telescope site already aligned. Each assembled subsystem, 2 collimators and 2 cameras, was interferometrically checked for wavefront quality. Double path tests with null lenses and measured wavefront errors are discussed. The system spectral performance was fine tuned using a test fiber slit to achieve required resolution across the field of view. The absolute transmittance of the spectrograph bulk optics was measured in both blue and red channels over wavelength and compared to the predicted values.

Keywords: multi-object, spectrograph, IFU, fiber cable, alignment, interferometry, hexabundle, high multiplex.

1. INTRODUCTION

The Anglo-Australian telescope (AAT) is equipped with a range of instruments in the Cassegrain and prime focus. The multi-object two-degree-field facility (2df) allows to observe 400 objects simultaneously. A number of successful surveys have been completed and recent surveys are in progress[1]. Light from each object is captured by an individual fibre in the focal plane, which is suitable for both stellar and unresolved extended objects. A significant amount of galaxies and nebulae can be spatially resolved in the AAT prime focus opening up the possibility of radial velocity observations.

Hector is the new multi-object integral field instrument at the Anglo-Australian Telescope. It consists of the prime focus 2df positioner, two fibre cables feeding two spectrographs for an extragalactic survey. The Hector instrument increases 2df capabilities with the help of integral field units (IFUs) for extended objects. The primary objective of the new facility is spectroscopic observations of 15000 galaxies of the Southern sky.

Fibre based IFUs are widely used in applications where an image has to be split and each part processed in a separate spectral channel. Microlens arrays in front of fibres are used as 2D slicers of an original image[2,3]. This arrangement works particularly well for Cassegrain and Nasmyth foci because microlenses also convert slow telescope output (~ f/10 - f/15) into fast (~ f/3 – f/5) beam suitable for efficient guidance by fibres. In the prime focus of AAT, the telescope output is suitable for direct injection into fibres and microlens fore-optics can be omitted. Hector integral field units are

*ross.zhelem@mq.edu.au; phone 61 2 93724872; astralis.org.au/macquarie

Ground-based and Airborne Instrumentation for Astronomy IX, edited by Christopher J. Evans, Julia J. Bryant, Kentaro Motohara, Proc. of SPIE Vol. 12184, 1218475
© 2022 SPIE · 0277-786X · doi: 10.1117/12.2629649

hexagonally packed fibre arrays or hexabundles[4]. For Hector, there are 21 IFUs, namely, 14 x 61 fibres each, 2 x 37, 2 x 91, 1 x 127, 2 x 169. The largest hexabundle subtends 26" on the sky, the most frequently used one with 61 fibres covers 16", the fibre core is 1.6" in diameter.

The Hector positioner for IFUs was developed under constraint of limited space. The existing 2df facility has its own positioner integrated with the field and atmospheric dispersion corrector. The 2df positioner consists of two plates, one plate is deployed for observation and facing the telescope mirror and the other plate facing the sky and being configured for the next science field. The 2df plates are exchanged by tumbling the plate holder by 180 degrees. The Hector positioner plate is fit to operate at 90 degree of tumbler rotation. There is no room for a robot permanently installed on the tumbler, therefore, a field plate is configured by the Hector robotic positioner off the telescope, and magnetic holders for IFUs adhere to the plate in precise locations. Then the plate is installed on the telescope and IFUs are placed by an observer into kinematic seats of holders. The second Hector field plate is configured by the positioner during observation with the first one. The Hector positioner magnetic holders are designed to correct for telecentricity. This is an advantage in comparison with the 2df positioners that allows to eliminate geometric focal ratio degradation and maximize flux injected into hexabundles.

On the opposite end, the IFU fibres are terminated into slits feeding two spectrographs, namely, the existing AAOmega spectrograph and the new higher resolution Spector. The fibre cables are routed along the telescope and the dome to the spectrograph locations. The AAOmega cable carries 819 fibres and is ~ 40 meters long and Spector cable has 855 fibres and is ~ 60 meters long. Both cables include 90 sky fibres in addition to IFU fibres to measure sky background in the field of view.

The AAOmega spectrograph[5] is the workhorse of the 2df facility. It provides continuous spectrum over the range 370 – 880 nm at R=1400 and a range of higher resolutions up to R=11000 but with partial wavelength coverage. One of the AAOmega modes will be used for the red spectrum of the Hector extragalactic survey.

Spector is the new spectrograph designed[6,7] and built specifically for the Hector instrument. This is a fixed format, dual (blue and red channels) spectrograph covering the range 372 – 778 nm at R=4500. Spector is installed in an environmentally controlled room to ensure stability of optical performance. Both spectrographs are mounted on an optical bench.

2. SPECTOR OPTICS

Spector has an all refractive (Figure 1) optical design[6]. This approach allows to avoid off-axis reflection from a collimator mirror or beam obstruction if a collimator mirror is used on-axis. Anti reflective coatings can be made very efficient in the blue end of the wavelength range in comparison with mirror coatings. Before Spector, AAO designed and built a smaller spectrograph of half the size and resolution. Spector project followed up on this experience. The spectrograph design specifications have been investigated in details[7].

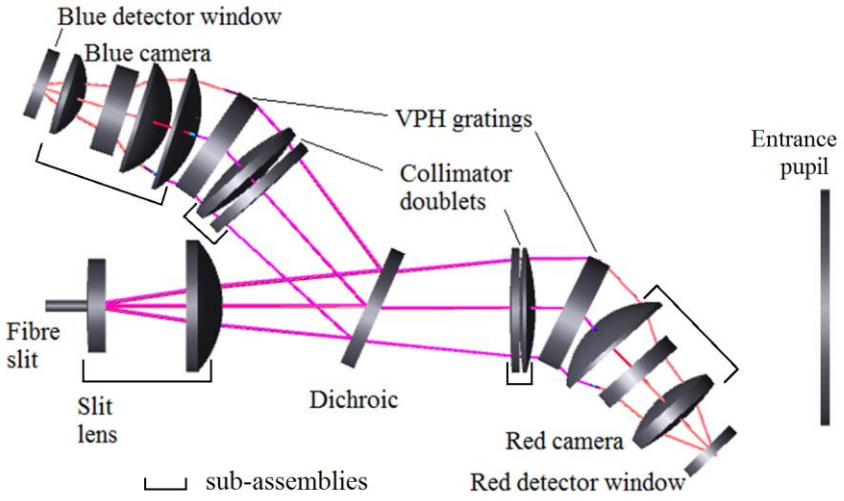

Figure 1. Optical layout of Spector. View on optical bench from above.

The entrance pupil is located on the primary optical axis which is defined by the collimator lens (between the slit lens and the dichroic beam splitter) in the center of curvature of the surface adjacent to the fibres. To form the pupil, the fibre pointing is adjusted at each field location to be perpendicular to the slit lens surface.

The spectrograph optics have been optimized for hexabundle input. Hexabundles are produced by arranging the fibres in hexagonal rings. In order to maximize the fill factor, the fibre cladding diameter is reduced by etching over a short distance. Then the etched sections are packed hexagonally and fused with interstitial holes packed with a low stress glue. The output energy distribution from mode coupling in any fibre results in a characteristic encircled energy profile of the beam emerging from the slit. An average radial profile was obtained from measurements and explicitly accounted for during spectrograph design. The Spector optics is fine tuned for the best performance with hexabundle input.

3. ALIGNMENT AND TESTING

The Spector assembly consists of individual elements (VPH gratings, dichroic beam splitter) and lens sub-assemblies (Figure 1). The common path optics are grouped together, the slit lens is removable and mounted on kinematic seats. The slit lens must be accessible for inspection of fibre-lens interface containing an optical gel for lossless coupling. The other four assemblies are collimator doublets, blue (4 lenses) and red (3 lenses) cameras. Each sub-assembly undergoes alignment and testing followed by the full system integration.

3.1 Lens-to-lens alignment

The spectrograph is optical table mounted and, in principle, all lenses could be attached to the table directly. However, a tolerance analysis revealed that lens-to-lens alignment has to be accomplished to within 15 micron in decentre for some camera lenses operating in the fast f/1.3 beam. Each camera has 3 aspheric lenses with surface departures 0.2-0.8 mm from the best fit sphere. Given the close separations between some lenses, e.g. elements of doublets, a standalone sub-assembly (Figure 2) on a lens centring station provides the required accuracy.

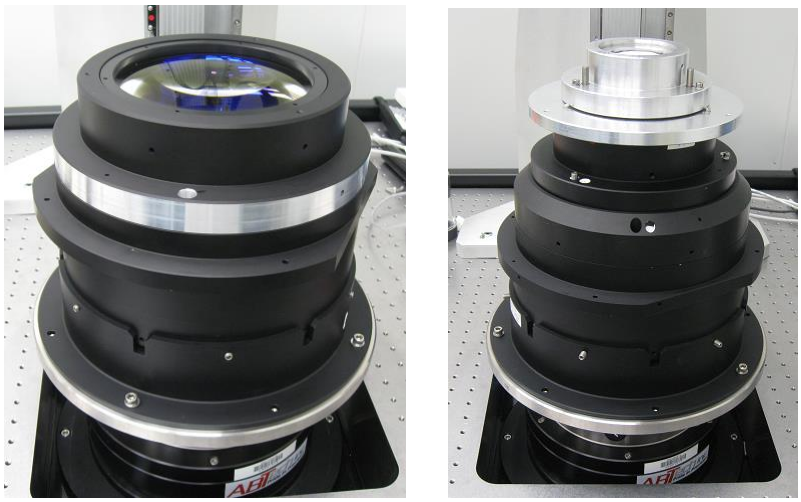

Figure 2. Lens sub-assembly. Left: stack build-up. Right: test lens integration.

The alignment process is based on a high precision air-bearing stage with negligible runout error (< 2 micron). The axis of rotation of the stage becomes the optical axis of a lens assembly. Each lens is aligned to the axis of rotation in tilt and decentre. The centres of curvature of both surfaces of a lens are viewed at high magnification so that they rotate in the field of view of a microscope until co-aligned with the optical axis. This is achieved by iterative adjustment of the lens. The separation between the lenses is measured by the same microscope mounted on a vertical stage with digital readout. An aligned lens is potted in its cell with RTV around the edge, the cell is potted with respect to the previous cell by a CTE matching epoxy. The entire lens stack can be disassembled if necessary.

An interferometric test lens complements a camera assembly (Figure 2). The test lenses for the Spector assemblies are compact because they work in the convergent beam close to focus (Figure 4). It is critically important that they are aligned with the rest of the system to the same high tolerances and do not contribute misalignment error to wavefront measurements. This is straightforward when a test lens is aligned in the same setup.

3.2 Slit assembly

Axially symmetric systems are commonly affected by barrel or pincushion distortion. Both kinds of distortion maintain axial symmetry. Spectrographs are subject to plane symmetric distortion that results in the shift of a spectrum in dispersion direction for off-axis field points. This effect, also known as spectral smile, can be tracked to a diffraction grating (or prism) introducing asymmetry along the dispersion direction. A linear slit acquires a curvature on a detector when imaged by a spectrograph in monochromatic light. Data acquisition system routinely corrects for spectral curvature but the fit of the spectrum into the detector active area will result in loss of spectral resolution. The Spector slit is curved in the opposite direction (Figure 3, left) yielding a straight monochromatic image.

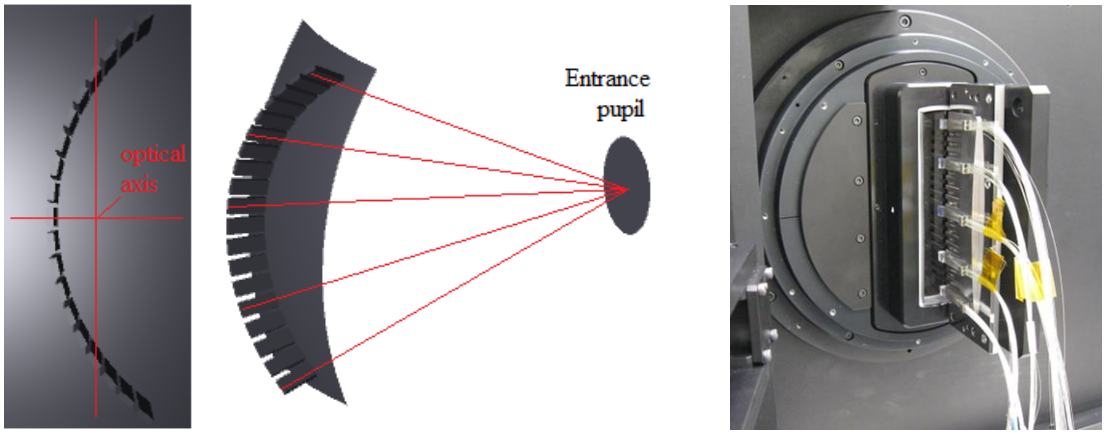

Figure 3. Spector slit design. Left: slitlet configuration (exaggerated for clarity). Right: slit body with 5 test slitlets.

The Spector slit consists of 19 slitlets each with 45 fibres in parallel V-grooves. The front face is tangent to the slit lens and the central fibre of a slitlet is pointing to the entrance pupil. The slit geometry is precision machined in the slit body (Figure 3, right). Each slitlet is mounted into a seat of the slit body, optical gel is applied and the slitlet slides until butted against the slit lens. All slitlets are assembled on manufacturing tolerances. Pointing of slitlets was verified with respect to the design location of the entrance pupil.

The slit mount is adjustable in the spectral direction and the central slitlet is translated to the design offset from the optical axis. Slit rotation is set as-built and becomes the reference (Section 3.4) for alignment of gratings and detectors in roll.

3.3 Sub-system interferometry

Wavefront performance of each sub-system was measured in order to verify that the assembly process was successful and units are ready for system integration. Collimators can be tested without the slit lens and cameras can not include the detector window which is the part of the detector assembly. Therefore, null lenses are made for double pass interferometric tests (Figure 4, left). An interferometer with f/0.8 transmission sphere forms the test beam at input and the collimated output is returned by a precision flat mirror. Both cameras are tested in equivalent f/1.0 beam to cover full effective area of the front lens surface.

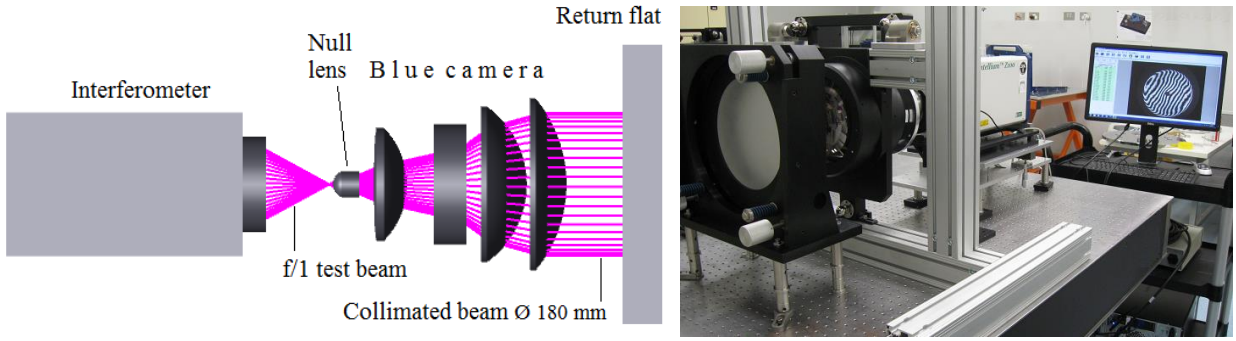

Figure 4. Blue camera interferometry. Left: optical layout. Right: lab setup.

The cameras are complete assemblies so they are tested in a dedicated setup (Figure 4, right). Collimators are integrated and tested directly on the spectrograph structure with null lenses mounted in place of the slit lens.

Null lenses are designed for highly aspheric surfaces correcting aberrations up to the 9th order. The lenses have the simplest plano-spherical shape and correct the majority of wavefront. For full correction, a complex multi element lens would be needed which is not practical. Direct wavefront measurements are limited by the residual error of a null system design.

Interferometric tests are usually designed on-axis and consequently, they are very field dependent. Field aberrations increase very fast and additional alignment efforts are necessary to minimize and then remove them. For Spector assemblies, the optical axis was determined at the stage of precision alignment (Figure 2), materialized by fiducials and used to setup on-axis wavefront metrology.

Table 1. Wavefront contributions (peak-to-valley) of elements and assemblies in waves at 632.8 nm

Spectrograph channel	Collimator	Dichroic	VPH	Camera	Spector design
Blue	0.53/0.49	0.18	2.9	0.40/0.38	4.5
Red	0.9/0.35	0.15	2.8	0.65/0.28	

Wavefront measurements are summarized in Table 1. All data are taken with an 632.8 nm interferometer and should be scaled to any other wavelengths. The dichroic beamsplitter and VPH gratings were characterized earlier[7]. Two measured values are available for the beamsplitter, namely, in reflection from the splitting surface and in transmission through both surfaces. For collimator and camera the measured wavefront is followed by the residual error of null lens design. All contributions are less than the wavefront error of spectrograph optical design.

3.4 System alignment

The spectrograph is aligned with respect to the primary optical axis which is defined by the slit assembly. The fibre slit and the slit lens is removed and the axis is established by an alignment telescope by viewing the collimator lens. All the optics are placed at a design angle and separation using this reference (Figure 5, left). To reproduce the folded configuration, a digital goniometer is placed on the optical axis at the point of intersection with an optical axis of an assembly. Then the goniometer rotates a flat mirror by a specified angle to 3" accuracy and the folded optical path is observed in the alignment telescope. Distances are measured with an inside micrometer.

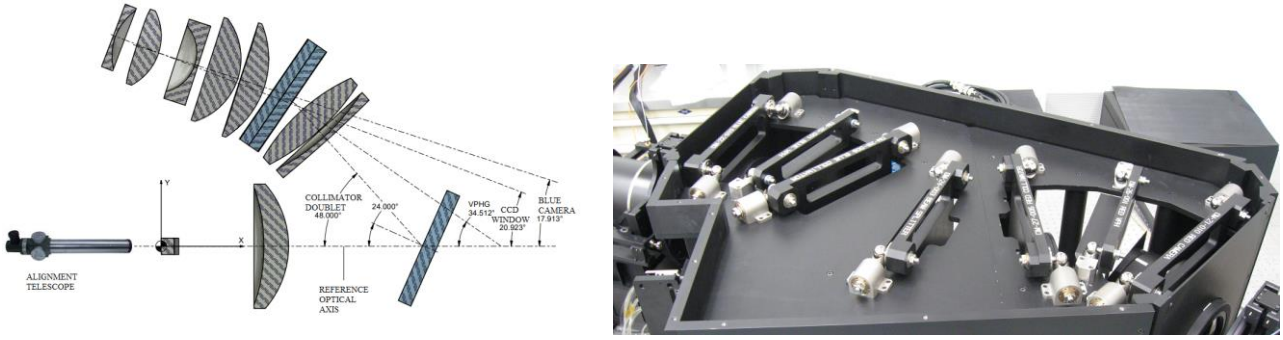

Figure 5. Spectrograph alignment. Left: alignment diagram. Right: adjustable kinematic mounts.

Each element or assembly is aligned with respect to a folded optical axis with the help of adjusters integrated into the cells and holders. In order to align the next optics, we need clear line of sight in the alignment telescope and the previously aligned optics have to be removed. For accurate replacement of aligned components, all mounts are equipped with kinematic seats (Figure 5, right) due to which the alignment accuracy is maintained and can be recovered after disassembly and separate storage of optics. Final system assembly occurs shortly after all optical elements and sub-assemblies have been aligned individually to the common reference.

3.5 Image fine tuning

Detectors are tilted and decentered with respect to the cameras. The detector windows are powered lenses making spectra sensitive to translational errors. The alignment of the detectors is finalized on test spectra. A test slit (Figure 3) with 5 slitlets (out of 19) covering the full length was used for lab alignment. The detectors are mounted on adjustable stages for precise positioning and focusing.

The slit rotation is fixed (Section 3.2). The orientation of spectra is affected by the direction of grating dispersion and pixel grid. First, the rotation of a grating is set to make spectra perpendicular to the slit, then the detector grid is adjusted in roll to become square to the spectrum.

The detector windows are mounted externally with some practical tolerances with respect to the detector and the spectrum may be shifted significantly. With the powered window, a simple translation of the detector assembly is not sufficient to compensate for that. The camera field angle has to be adjusted which implies that simultaneous tilt of camera and detector has to be implemented. This is achieved with the help of fine tilt mechanisms on both assemblies.

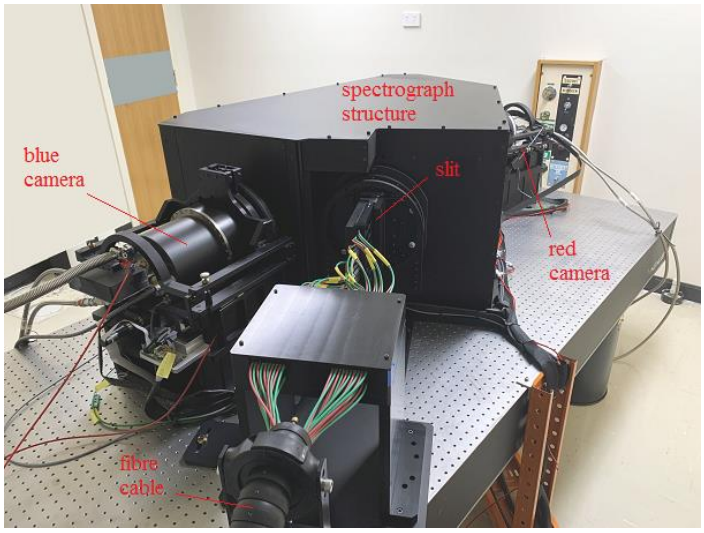

Figure 6. Spector installed at the Anglo-Australian telescope.

After laboratory alignment and throughput metrology (Section 4), the spectrograph was moved to the telescope site. All optical elements and assemblies were shipped in their holders with kinematic mounts, the spectrograph structure was shipped assembled to keep all kinematic mounts in the same location. Upon reassembly at site, all the optics inside the spectrograph structure (Figure 6) were mounted directly and did not require the full alignment procedure (Section 3.4) to be repeated. The full science slit was connected to the spectrograph input for the first time and the cameras fine tuned for the best performance across the field of view.

4. OPTICAL PERFORMANCE

The spectral resolution was predicted at the stage of spectrograph optical design (Figure 7). The resolution element refers to the full width of half maximum of a monochromatic fibre image collapsed in the spatial direction. The resolution element is almost constant in comparison with design spectral resolution $R=\lambda/\Delta\lambda$ which is proportional to the wavelength. The measured values are influenced by as-built aberrations of optical elements and assemblies (Table 1).

The resolution in the spatial direction depends on the separation between the fibres in the slit. Close fibre separation is beneficial from a packaging standpoint. At the same time, the cross talk between adjacent spectra increases and it is important to reliably extract the spectra during data processing. Simulated spectra were generated at different separations and reduced by the standard software tool. The success of data processing is the criterion for minimum fibre separation. The algorithm turned out to be capable of extraction spectra at 3 pixel separation on the detector. Given the total amount of fibres and the length of the slit, the separation was set to 4.6 pixels (this corresponds to 164 micron in a slitlet vs 123 micron fibre cladding diameter). Data reduction software developed for simulated spectra, was directly applied to real frames and succeeded to extract multi-object spectra.

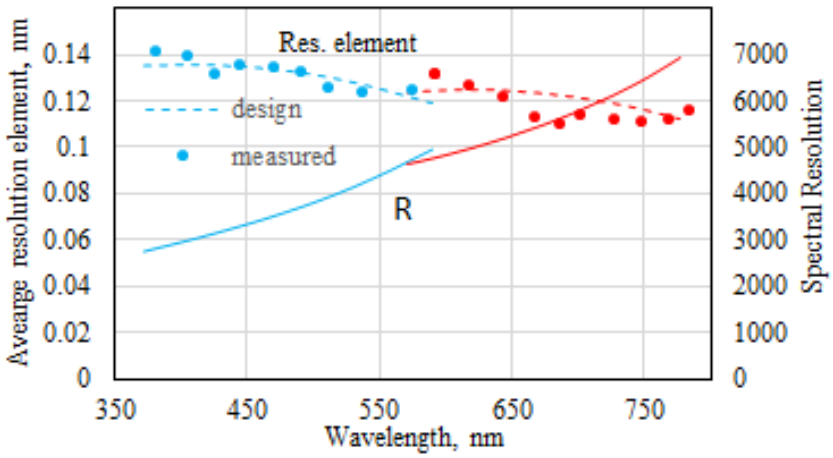

Figure 7. Spectral resolution vs wavelength: design and measurements.

Spector throughput was also predicted[7] based on measured reflectance of AR coatings, VPH grating throughput and quantum efficiency of detectors. Throughput of the assembled spectrograph was measured from the slit lens to the last lens of each camera (Figure 8). The raw data were corrected for Fresnel reflection of the first surface of the slit lens and losses on camera windows were added. Detector quantum efficiency data were interpolated between the measured points. The peak efficiency of the spectrograph optics exceeds 70%.

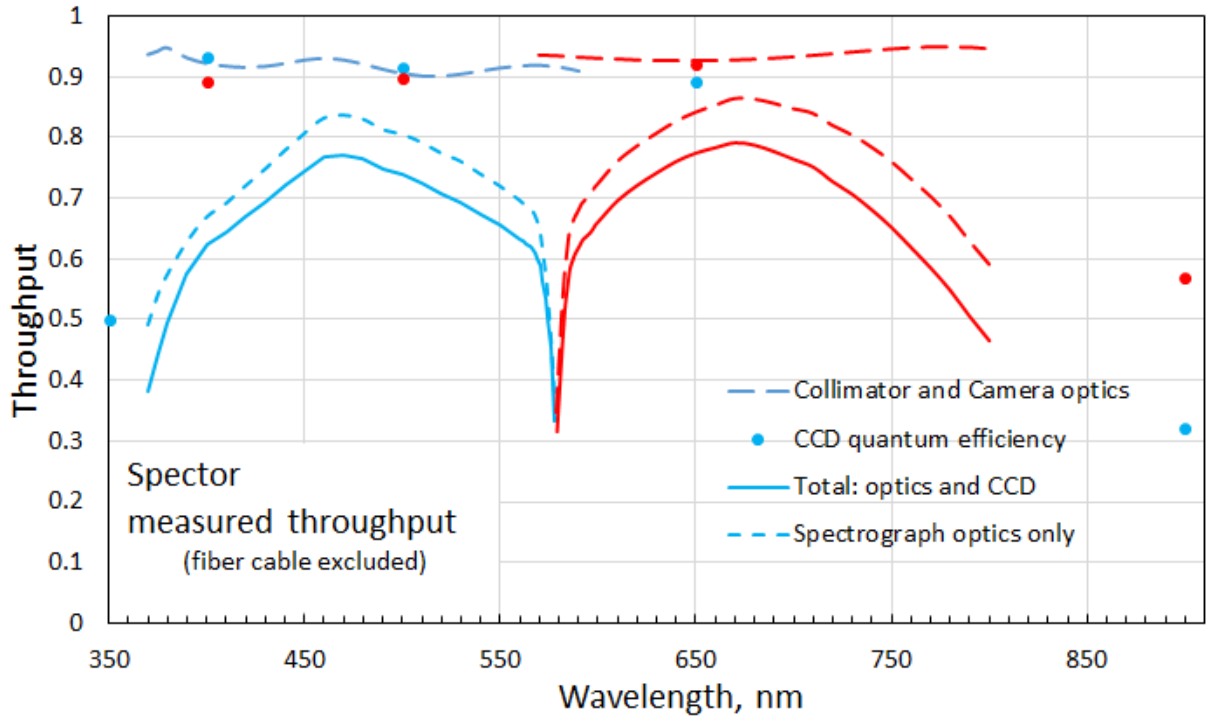

Figure 8. Spectrograph throughput from slit lens to detectors.

Throughput measurements include only bulk optics of the spectrograph. Neither fiber cable, hexabundles, prisms, sky transmission at the site, telecentricity correction losses nor the losses due to focal ratio degradation are included into the measurement. The test beam was formed by a spot projector, made slightly undersized (f/3.7) in comparison with nominal fibre output (f/3.3) and aligned to clear pupil stops in the system. The measured throughput is determined by the properties of optical coatings and diffraction efficiencies of VPH gratings.

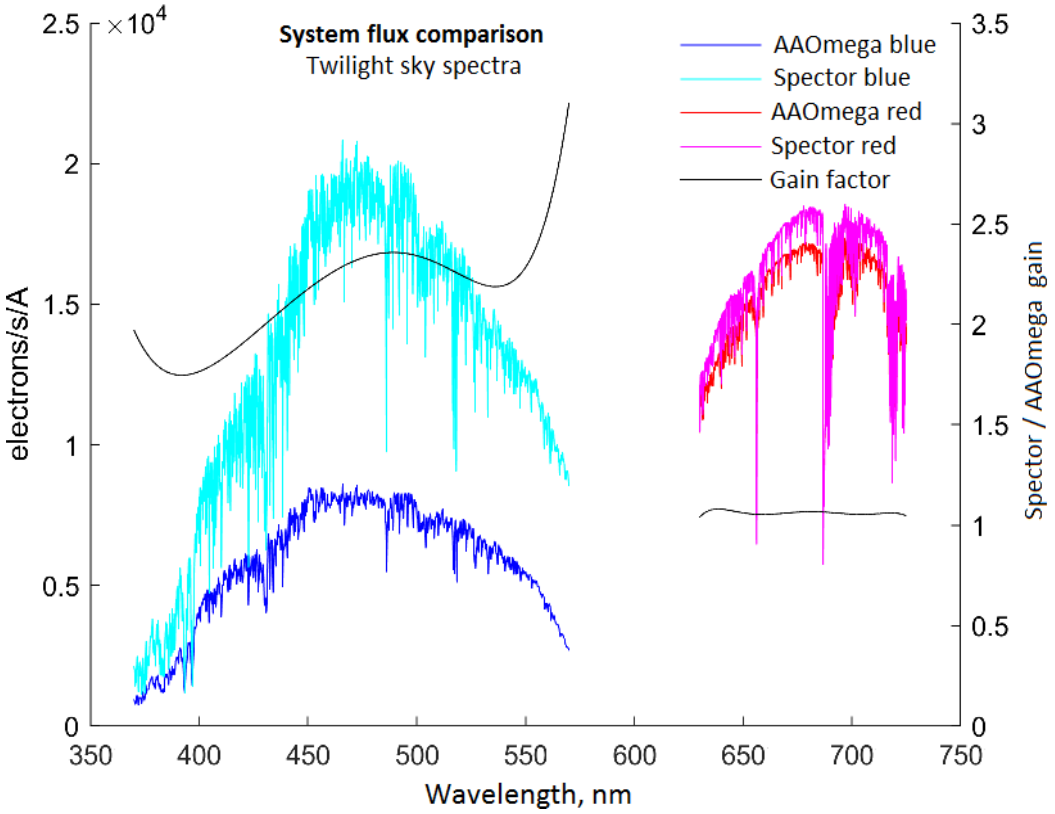

Figure 9. End-to-end flux of Hector spectrographs.

The spectra of twilight sky were taken by both spectrographs of the Hector instrument (Figure 9) for flux comparison. The fibre cables are different for AAOmega and Spector but they are made of the same fibre and IFU technology. The gain in end-to-end throughput is up to 3 times higher for Spector in the blue channel. The peak flux of Spector blue channel is higher than that of the red channel in agreement with shorter wavelengths dominating twilight due to Rayleigh scattering in the atmosphere.

CONCLUSIONS

Spector has been tested on sky and proved to deliver expected spectral and spatial resolution. Data reduction software has been calibrated and extracts science spectra for all fibre sources within design wavelength coverage. Spector would benefit from diffraction gratings with lower wavefront contribution, this should be traded against diffraction efficiency.

Spector features very efficient bulk optics capable of peak throughput over 70%. Similar high quality optics should be used in future spectrographs for the best signal to noise ratio.

Spector is optimized for the best performance with hexabundle IFUs. The spectrograph optical design is very flexible to work with any fibre fed input in a variety of applications.

Spector delivers up to 3 times more flux in the blue channel than the AAOmega spectrograph. The Spector design can be extended to a 3 channel instrument covering full wavelength range out to 1 micron with fixed format.

REFERENCES

[1] Buder, S., Sharma, S., Kos, J., Amarsi, A. M., Nordlander, T., Lind, K., Martell, S. L., Asplund, M., Bland-Hawthorn, J., et. al., " The GALAH+ survey: Third data release," Monthly Notices of the Royal Astronomical Society 506(1), 150-201 (2021).

[2] Zhelem, R., Brzeski, J., Case, S., Churilov, V., Ellis, S., Farrell, T., Green, A., Heng, A., Horton, A., Ireland, M., Jones, D., Klauser, U., Lawrence, J., Miziarski, S., Orr, D., Pai, N., Staszak, N., Tims, J., Vuong, M., Waller, L. and Xavier, P., "KOALA, a wide-field 1000 element integral-field unit for the Anglo-Australian Telescope: assembly and commissioning," Proc. SPIE 9147, Ground-based and Airborne Instrumentation for Astronomy V, 91473K (2014).

[3] Sheinis, A. I., Anthony, A., Baker, G., Burley, G. S., Churilov, V., Edgar, M., Ireland, M., Kondrat, Y., Pazder, J., Robertson, G., Young, P. G., and Zhelem, R., "The Gemini High-Resolution Optical SpecTrograph (GHOST)," Proc. SPIE 9908, Ground-based and Airborne Instrumentation for Astronomy VI, 990817 (2017).

[4] Bland-Hawthorn, J., Bryant, J. J., Robertson, G., Gillingham, P., O'Byrne, J., Cecil, G., Haynes, R., Croom, S., Ellis, S., Maack, M., Skovgaard, P., Noordegraaf, D., "Hexabundles: imaging fiber arrays for low-light astronomical applications," Optics Express 19, 2649 (2011).

[5] Saunders, W., Bridges, T., Gillingham, P., Haynes, R., Smith, G. A., Whittard, J. D., Churilov, V., Lankshear, A., Croom, S., Jones, D. and Boshuizen, C., "AAOmega: a scientific and optical overview," Proc. SPIE 5492, Ground-based Instrumentation for Astronomy, (2004).

[6] Content, R., Saunders, W., Lawrence, J., Bryant, J. and Zhelem, R., "Optical design of the highly cost optimized new Hector Spectrograph," Proc. SPIE 10702, 107028I (2018).

[7] Zhelem, R., Content, R., Saunders, W., Lawrence, J., Zheng, J., Bryant, J., Bland-Hawthorn, J., Robertson, D., Mohanan, M. and Venkatesan, S., "The Hector Instrument: optical design of the new higher-resolution spectrograph," Proc. SPIE 11447, Ground-based and Airborne Instrumentation for Astronomy VIII, 114478U (2020).